

## Article

# Investigating the Influence of All-Ceramic Prosthetic Materials on Implants and Their Effect on the Surrounding Bone: A Finite Element Analysis

Saniya Juneja <sup>1</sup>, Glynis Miranda <sup>2</sup>, Afiya Eram <sup>3</sup> , Nisha Shetty <sup>4</sup>, Chethan K N <sup>5,\*</sup>  and Laxmikant G. Keni <sup>5,\*</sup> 

<sup>1</sup> Prosthodontist and Head Saffron Dental Clinic and Implant Center, New Delhi 110005, India; saniyajuneja@gmail.com

<sup>2</sup> A.J. Institute of Dental Sciences, Kuntikana, Mangalore 575004, Karnataka, India; dr.glynis@gmail.com

<sup>3</sup> Department of Conservative Dentistry and Endodontics, Manipal College of Dental Sciences, Manipal Academy of Higher Education, Manipal 576104, Karnataka, India; afiya.eram@manipal.edu

<sup>4</sup> Department of Oral Pathology and Microbiology, Manipal College of Dental Sciences, Manipal Academy of Higher Education, Manipal 576104, Karnataka, India; nisha.rai@manipal.edu

<sup>5</sup> Department of Aeronautical and Automobile Engineering, Manipal Institute of Technology, Manipal Academy of Higher Education, Manipal 576104, Karnataka, India

\* Correspondence: chethan.kn@manipal.edu (C.K.N.); laxmikant.keni@manipal.edu (L.G.K.)

**Abstract:** This study aims to assess and compare the impact of Monolithic Zirconia (MZ) and In-Ceram Zirconia (ZP) superstructures on stress distribution within implants and D2/D4 bone densities under 200 N vertical and oblique occlusal loads using three-dimensional finite element analysis via ANSYS WORKBENCH R2. The analysis employed maximum and minimum von Mises stress values. Modeling an implant (4.2 mm diameter, 10 mm length) and abutment (0.47 mm diameter), with an 8 mm diameter and 6 mm length single crown, the research identified lower von Mises stresses in D2 cancellous bone with the MZ model under vertical loading. Conversely, under oblique loading, the ZP model exhibited maximum von Mises stresses in D4 bone around the implant. This underscores the critical need to consider physical and mechanical properties, beyond mere aesthetics, for sustained implant success. The findings highlight the effect of material composition and stress distribution, emphasizing the necessity of durable and effective implant treatments.

**Keywords:** monolithic zirconia; ceramic zirconia; finite element analysis; von Mises stresses; D2/D4 bone



**Citation:** Juneja, S.; Miranda, G.; Eram, A.; Shetty, N.; K N, C.; Keni, L.G. Investigating the Influence of All-Ceramic Prosthetic Materials on Implants and Their Effect on the Surrounding Bone: A Finite Element Analysis. *Prostheses* **2024**, *6*, 74–88. <https://doi.org/10.3390/prostheses6010006>

Academic Editors: Andrea Scribante, Maurizio Pascadopoli and Simone Gallo

Received: 30 November 2023

Revised: 29 December 2023

Accepted: 4 January 2024

Published: 17 January 2024



**Copyright:** © 2024 by the authors. Licensee MDPI, Basel, Switzerland. This article is an open access article distributed under the terms and conditions of the Creative Commons Attribution (CC BY) license (<https://creativecommons.org/licenses/by/4.0/>).

## 1. Introduction

Implants have revolutionized the field of dentistry by providing a reliable and long-term solution for replacing missing teeth. Advancements in implant technology, materials, and techniques have significantly enhanced their success rates [1,2]. Improvements in implant materials, such as the development of titanium alloys, have made implants more durable and biocompatible, reducing the risk of rejection or failure [3]. Additionally, advancements in imaging technology, like 3D imaging and computer-guided implant placement, allow for the more precise planning and placement of implants, which contributes to their success [4]. The cervical area, where the crown meets the root of a natural tooth, plays a significant role in the appearance and function of the tooth. Mimicking this area in dental implants involves creating a seamless transition from the implant fixture to the prosthetic crown. This not only contributes to a more natural appearance but also helps in maintaining healthy gum tissue and proper function during biting and chewing. Creating implants that closely resemble natural teeth, especially in the critical cervical area, contributes not only to the patient's satisfaction but also to the long-term success and stability of the implant restoration.

The maxilla (upper jaw) and mandible (lower jaw) exhibit distinct physical characteristics in terms of their structure and density, which have implications for implant placement and treatment outcomes. The classification of bone quality, as outlined by Lekholm and Zarb,

categorizes bone density into four types: D1, D2, D3, and D4. This classification system helps in understanding the bone characteristics at potential implant sites [5]. The mandible is said to have D2 bone quality and the maxilla has D4 bone quality. The mandible has a higher proportion of cortical bone (dense outer layer) compared to the maxilla, which contains more cancellous or trabecular bone (spongy inner bone). The cortical bone offers better primary stability for implants, thus requiring less bone grafting or additional procedures to support the implant in the mandible. The maxilla's cancellous bone might necessitate additional care during implant placement to ensure stability [6]. The difference in bone quality between the maxilla and the mandible, with the mandible typically having denser bone quality, influences the treatment approach and considerations during implant placement.

The decision to select the prosthetic framework involves considering various factors to ensure the long-term success, stability, functionality, and aesthetics of the restoration [7,8]. Metal–ceramic combinations have traditionally been used due to their strength, durability, and satisfactory aesthetics. However, with advancements in material science, zirconia, a type of ceramic, has gained popularity for its improved strength and aesthetics [9,10]. Zirconia restorations offer high biocompatibility and excellent mechanical properties, making them suitable for certain implant-supported prostheses [11,12].

Zirconium oxide, commonly referred to as zirconia, has gained significant popularity in dentistry due to its excellent properties and versatility in various dental applications [13]. Zirconia is currently used as a core material for the fabrication of prosthetic frameworks for teeth and implant-supported fixed partial dentures. In addition, zirconia is considered more biocompatible than other ceramics, titanium, and metal alloys, which may facilitate soft tissue responses in terms of health [14]. With increasing public demand for aesthetically pleasing restorations, there has been an increase in the application of all ceramic restorations, with yttria-stabilized tetragonal zirconia polycrystal being one of them since it has higher flexural strength (800–1500 MPa) and fracture resistance [15]. Since zirconia ceramics are opaque, to make them more aesthetically pleasing, it is covered by a layer of glass ceramic. The zirconia full-coverage crown without veneering dental porcelain has the advantage that no dental porcelain is fractured due to the absence of an upper structure, and hence it is preferred in areas of high masticatory load. Since clinical studies have shortcomings, finite element analysis (FEA) is a numerical stress analysis technique that has proven to be a useful tool in investigating the effect of the biomechanical properties of prostheses on dental implants [16]. Several in vitro studies and FEA were conducted to explore stress transmission at both the implant and peri-implant levels, employing various restorative materials for implant-supported prostheses [17–21]. This study was conducted to evaluate and compare the effect of monolithic zirconia and In-Ceram zirconia superstructures on the distribution of stresses in implants and D2 and D4 bone densities after the application of a vertical and oblique occlusal load of 200 N with the aid of a three-dimensional finite element study. Stress levels were calculated using maximum and minimum von Mises stress values.

## 2. Materials and Methods

### 2.1. Modeling

Patients with a partially edentulous condition, such as missing second molars, underwent a CT scan of the maxilla and the mandible which was adopted for the 3D modelling of maxillary and mandibular bone. A 3D slicer-free, open-source software was used to build the model for the CT. The developed model was transferred to CATIA-3D EXPERIENCE R2019x software for further editing. The maxillary bone was modelled as a cancellous core D4 bone surrounded by a 1 mm thick cortical layer. The mandibular bone was modelled as a cancellous core D2 bone surrounded by a 2 mm thick cortical layer [Figure 1a,b]. From the CATIA-3D EXPERIENCE R2019x software, not only were the models edited, but solid models such as implant body, abutment, framework and occlusal surfaces were also created, as shown in Figure 2a–c. An implant measuring 4.2 mm in diameter and 10 mm in length

and an abutment measuring 0.47 mm in diameter were scanned and modelled as shown in Figure 2b.

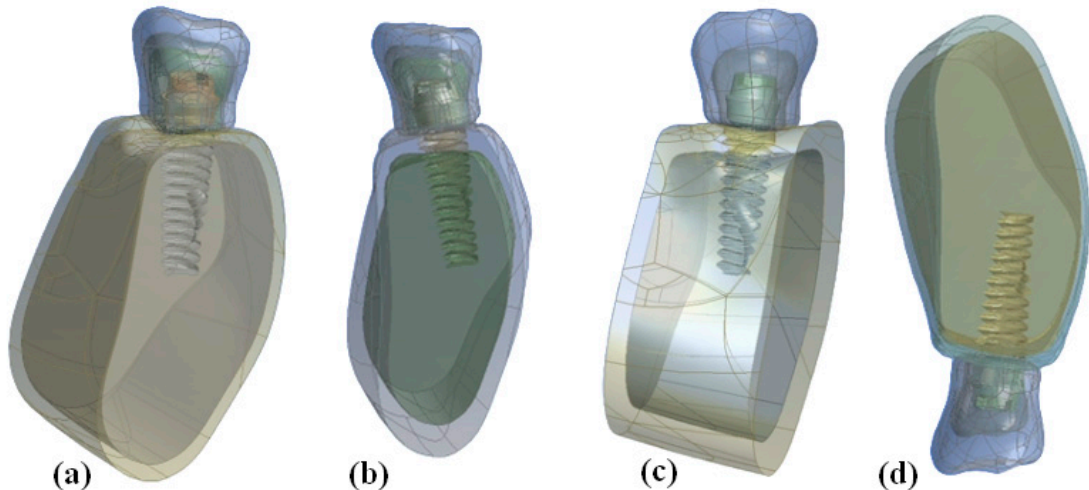


**Figure 1.** (a) Zirconia framework with porcelain veneering D4 bone. (b) Zirconia framework with porcelain veneering D2 bone. (c) Monolithic Zirconia-D4 bone. (d) Monolithic Zirconia-D2 bone.

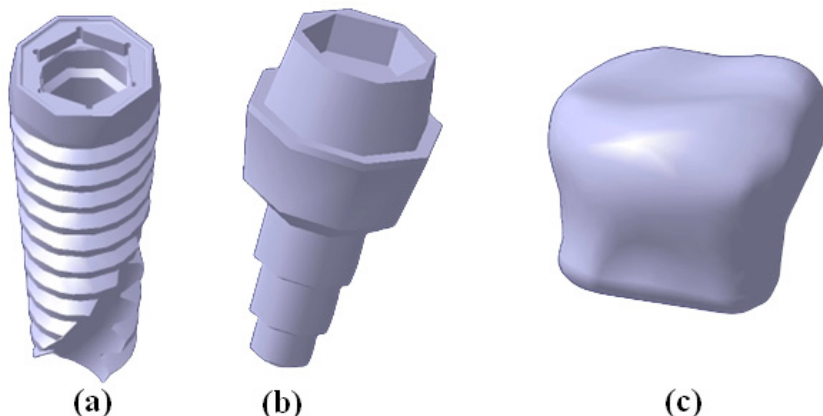


**Figure 2.** (a) Implant body. (b) Abutment model. (c) Crown.

A crown selected with an 8 mm length and 6 mm diameter was also modelled. The geometry of the tooth models was compared with data from *Wheeler's Dental Anatomy, Physiology, and Occlusion* [22] [Figure 2c]. Cement layer of 25 micron thickness was also modelled. The ZP model consisted of an In-Ceram zirconia framework and porcelain veneer. The design of the frameworks respected the anatomical form of the final restoration, with an occlusal veneering thickness of 2 mm. The frameworks were customized with a minimum thickness of 0.8 mm. Feldspathic porcelain (Ceramco11, Dentsply, Burlington, NJ, USA) was used for the occlusal surfaces. The MZ (monolithic zirconia) model consisted of only a monolithic zirconia framework with a minimum thickness of 2.8 mm, as shown in Figure 1c,d. The frameworks were developed as per the manufacturer's instructions. By using the ANSYS Workbench R2, the solid models were analyzed for stress and deformation.

## 2.2. Meshing and Boundary Conditions

In this study, numerical models of the crown–implant–bone assembly were generated using 4-node tetrahedral elements using ANSYS Workbench 2023 R2, a 3D finite element analysis software. The mesh convergence was carried out by varying the mesh size from 1 mm to 0.1 mm with an interval of 0.1 mm. It was observed that there was no significant difference in von Mises stresses, with a mesh size of less than 0.4 mm. So, it was finalized

with a mesh size of 0.4 mm for all the further analysis. Figure 3b shows the mesh convergence study. The number of nodes and elements in the final model is given in Table 1. Figure 3a shows the meshed models of the D4 and D2 bone models, respectively.

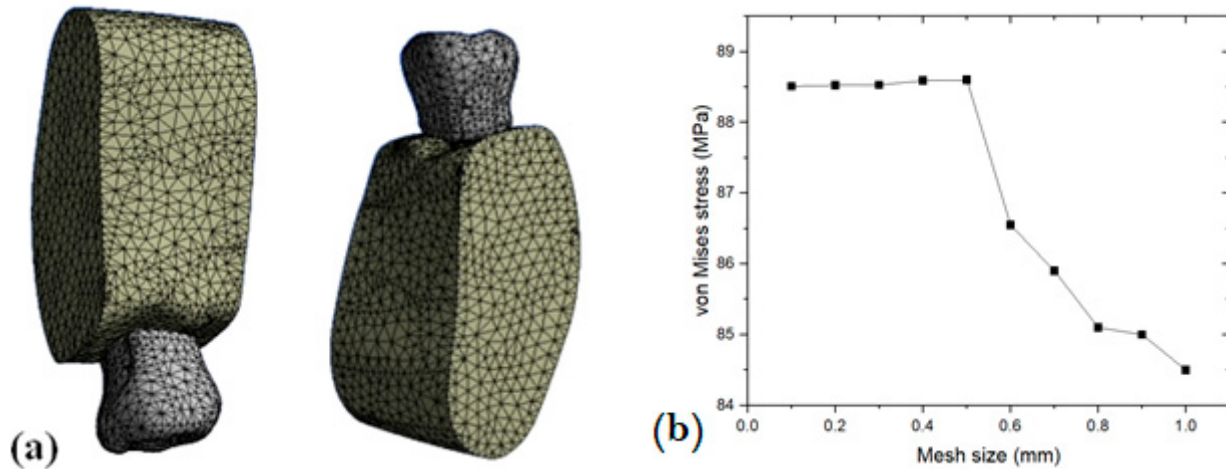


**Figure 3.** (a) Meshed models of D4 and D2 bone models; (b) mesh convergence study.

**Table 1.** Details of models and corresponding nodes and elements for each model.

Crown	Bone	Node	Elements
ZP	D2	92,687	52,158
MZ	D4	84,379	47,321

The analysis assumed that all materials were homogenous, isotropic, and exhibited linear elastic behavior. The model incorporated Poisson's ratio and modulus of elasticity for the respective materials, which were determined based on values obtained from literature sources (Table 2). These mechanical properties were utilized to accurately represent the material behavior within the simulation model.

**Table 2.** Mechanical properties.

Anatomic Structure	Modulus of Elasticity (GPa)	Poisson's Ratio	References
Implant	110	0.35	[23]
Abutment	110	0.28	[23]
Cement	12	0.35	[24]
Crown structure (ZP)	210	0.33	[15]
Crown structure (MZ)	210	0.3	[25]
Cortical bone (D2)	13.7	0.3	[23]
Porcelain	82.8	0.35	[26]
Cancellous Bone (D2)	1.37	0.3	[27]
Cancellous Bone (D4)	1.10	0.3	[23]

In the current study, a static load of 200 N was applied to the occlusal surface of the tooth model in both vertical and oblique directions [28] [Figure 4a,b]. This load was based on data obtained from previous works in the literature ([29,30]) and was applied as per the specifications outlined in Table 3. The base of the mandible and maxilla bone was fixed in all degrees of freedom, as shown in Figure 4a,b.

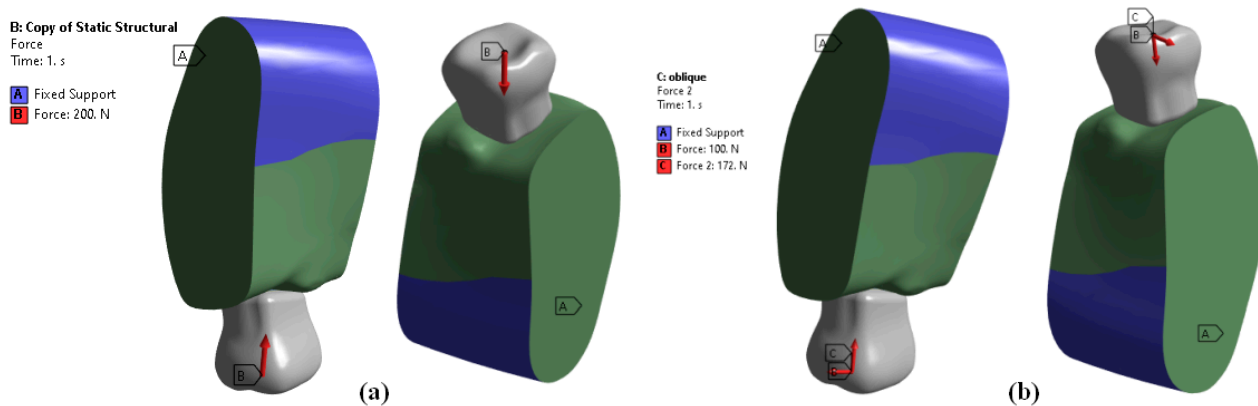


**Figure 4.** Boundary conditions applied: (a) vertical load; (b) oblique load.

**Table 3.** Loading condition.

Loading Condition	Magnitude of Load (N)	Direction
Static	200	Vertical
		Oblique ( $30^\circ$ to vertical)

### 3. Results

Four 3D finite element models were built with 3D modelling software (CATIA-3D EXPERIENCE R2019x) to analyze the stress distribution in two different bone densities with three different all-ceramic superstructures. Out of the four models, two models were used to calculate stress distribution in D2 bone and the other two models were used to calculate stress distribution in D4 bone. For each bone density, the two models were MZ (monolithic zirconia) and ZP (zirconia framework with porcelain veneering). Each set of models contained a crown, a cement layer, an abutment, an implant, and surrounding bone, which received a 200 N occlusal load. Stress distribution in the implant and surrounding bone was analyzed using 3D Finite Element Software (ANSYS WORKBENCH 2023 R2). For each model, stress levels were calculated using maximum and minimum von Mises stress values.

In the present study, different all-ceramic materials, namely In-Ceram zirconia and monolithic zirconia, used in a single implant-supported prosthesis in two different bone densities under static functional forces, affected the stress concentration.

#### 3.1. Stress Distribution within the Implant

Regardless of bone density or loading forces (vertical or oblique), the maximum von Mises stresses were concentrated at the neck of the implant [Figure 5a,b]. This area tends to experience higher stress due to the mechanical forces transmitted during chewing or biting. Under vertical loading forces, the minimum stresses were concentrated at the first thread from the neck of the implant in all models. This area experiences lower stresses compared to other parts of the implant structure when subjected to vertical forces. Interestingly, for oblique loading forces, the minimum stresses were concentrated at the root apex (bottom) of the implant in all models [Figure 5c,d]. This indicates that under oblique loading, the stress distribution differs, with lower stresses observed at the root apex compared to other areas.

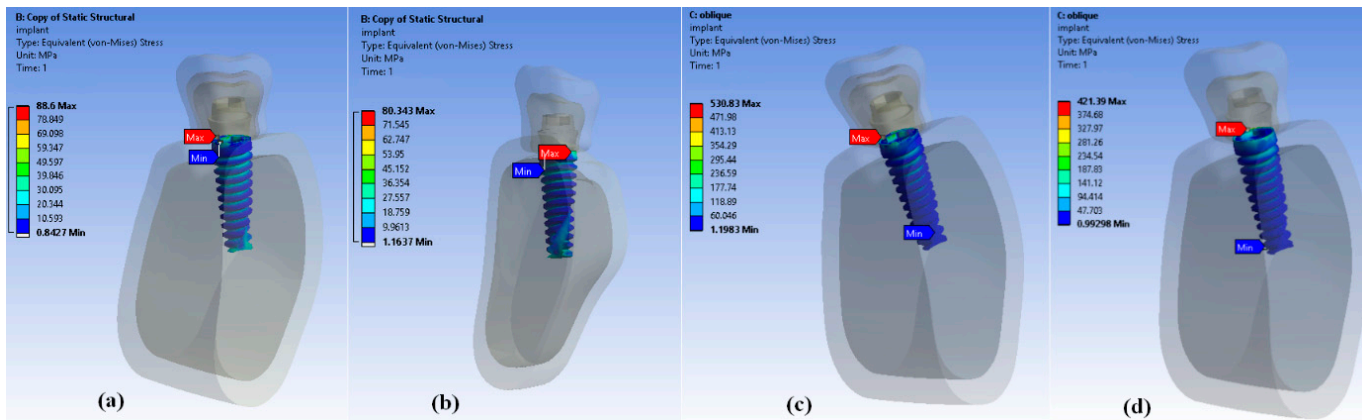


**Figure 5.** Stress distribution in D2 bone within the implant: (a) vertical loading in ZP and (b) vertical loading MZ models; (c) oblique loading in ZP and (d) oblique loading in MZ models.

The maximum von Mises stresses within the implant were 88.6 MPa for the ZP model and 80.34 MPa for the MZ model. These values represent the highest stresses experienced within the implant structure when subjected to vertical loading forces. Under oblique loading conditions, the maximum von Mises stresses within the implant were reported as 530.83 MPa for the ZP model and 421.39 MPa for the MZ model: Figure 5c,d. These stress values provide crucial information about the mechanical behavior and potential failure points within the implants under different loading scenarios, especially considering the bone density when classified as D2.

In scenarios involving D4 bone density, as shown in Figure 6a,b, the maximum stresses within the implant under vertical loading were reported as 116.24 MPa for the ZP model and 109.6 MPa for the MZ model. Under oblique loading conditions with D4 bone density, the maximum stresses within the implant were reported as 1099 MPa for the ZP model and 965.13 MPa for the MZ model, as shown in Figure 6c,d. The notably higher stress values under oblique loading compared to vertical loading in the context of D4 bone density highlight the increased susceptibility of implants to higher stresses when subjected to forces at an angle.

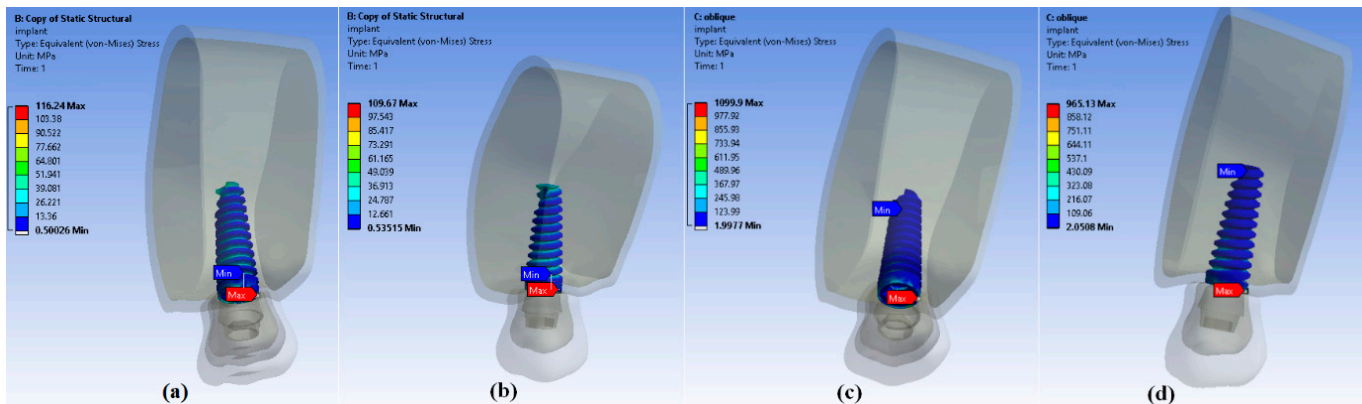


**Figure 6.** Stress distribution in D4 bone within the implant: (a) vertical loading in ZP and (b) vertical loading MZ models; (c) oblique loading in ZP and (d) oblique loading in MZ models.

### 3.2. Stress Distribution within the Supporting Bone of D2

Under vertical loading, the maximum stresses were observed in the cervical cortical bone region for all models (ZP and MZ). This area experienced the highest stress concentration when subjected to vertical forces. The maximum von Mises stresses observed in the cortical bone region were 21.77 MPa for the ZP model and 13.12 MPa for the MZ model [Figure 7a,b]. This indicates higher stresses in the cortical bone for the ZP model compared

to the MZ model under vertical loading conditions. The maximum stresses observed in the cancellous bone under vertical loading were 5.30 MPa for the ZP model and 4.41 MPa for the MZ model [Figure 7a,b]. Here, the ZP model also exhibited slightly higher stresses in cancellous bone compared to the MZ model under vertical loading conditions. Generally, higher stresses were seen in both models (ZP and MZ) under vertical loading compared to oblique loading forces in both cortical and cancellous bone regions. This indicates that the cervical cortical bone region experienced higher stress concentrations under vertical loading conditions compared to oblique loading conditions.

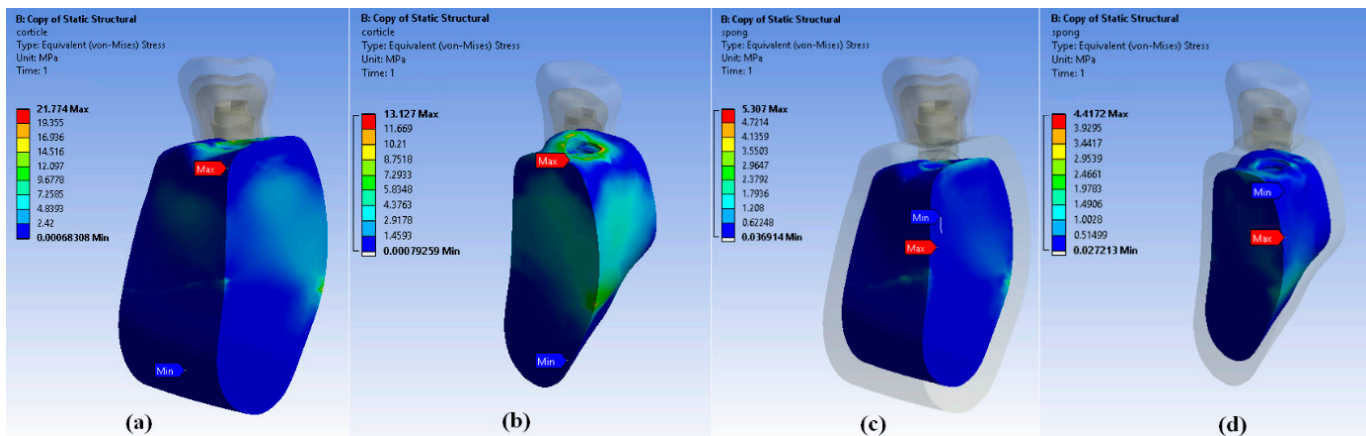


**Figure 7.** Stress distribution within supporting bone of D2 for vertical loading: (a) cortical bone in ZP and (b) cortical bone in MZ models; (c) cancellous bone in ZP; and (d) cortical bone in MZ models.

The maximum von Mises stresses were observed in both cortical and cancellous bone regions under oblique loading conditions for the ZP and MZ models. For the ZP model, the maximum von Mises stress observed in the cortical bone under oblique loading was 132.8 MPa. For the MZ model, the maximum stress observed in the cortical bone under oblique loading was 109.8 MPa [Figure 8a,b]. This indicates higher stress concentrations in the cortical bone for the ZP model compared to the MZ model when subjected to oblique loading forces.

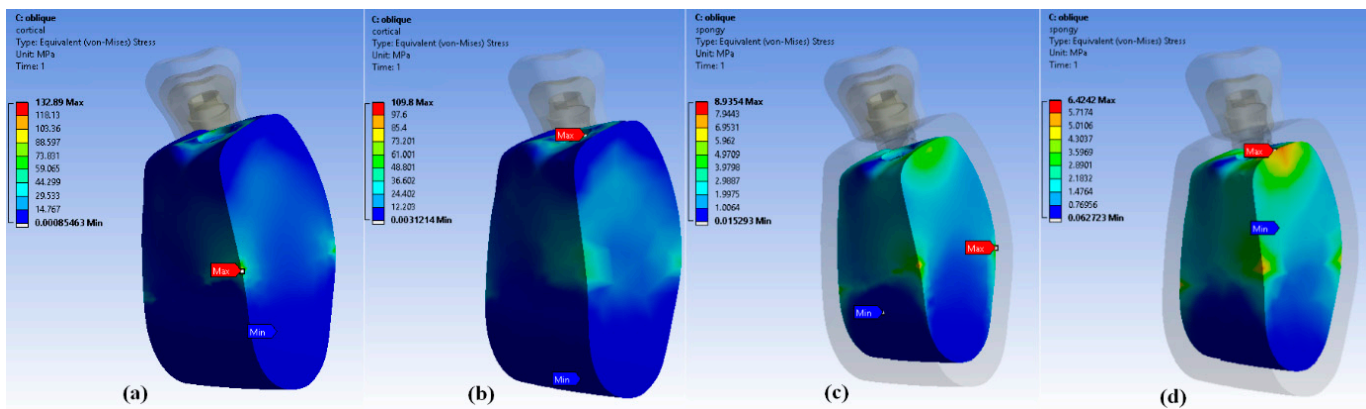


**Figure 8.** Stress distribution within supporting bone of D2 for oblique loading: (a) cortical bone in ZP and (b) cortical bone in MZ models; (c) cancellous bone in ZP; and (d) cortical bone in MZ models.

In the cancellous bone under oblique loading forces, the maximum stresses were 8.93 MPa for the ZP model and 6.42 MPa for the MZ model [Figure 8c,d]. Similar to the cortical bone, the ZP model exhibited higher stresses in cancellous bone compared to the MZ model under oblique loading conditions. These findings suggest that both cortical and cancellous bone regions experienced higher stress concentrations under oblique loading forces, and

the ZP model showed higher stress values compared to the MZ model in both types of bone tissues.

### 3.3. Stress Distribution within Supporting Bone of D4

Under vertical loading forces, the maximum von Mises stresses were observed in the cervical cortical bone region for all models (ZP and MZ). This area experienced the highest stress concentrations when subjected to vertical forces. The maximum von Mises stresses observed in the cortical bone region were 28.88 MPa for the ZP model and 25.65 MPa for the MZ model [Figure 9a,b]. This indicates higher stresses in the cortical bone for the ZP model compared to the MZ model under vertical loading conditions. Interestingly, for cancellous bone, all the models showed the same stress values for both vertical and oblique loading forces, with maximum stresses of 6.83 MPa [Figure 9c,d]. This suggests consistent stress levels in cancellous bone regardless of loading direction or model type. These findings provide valuable insights into the stress distribution within different bone regions (cortical and cancellous) under varying loading conditions and for different implant models. The information can be used for optimizing implant designs and selecting suitable implants to minimize stress concentrations and ensure long-term stability, especially considering the cervical cortical bone region's vulnerability to higher stresses under vertical loading forces.

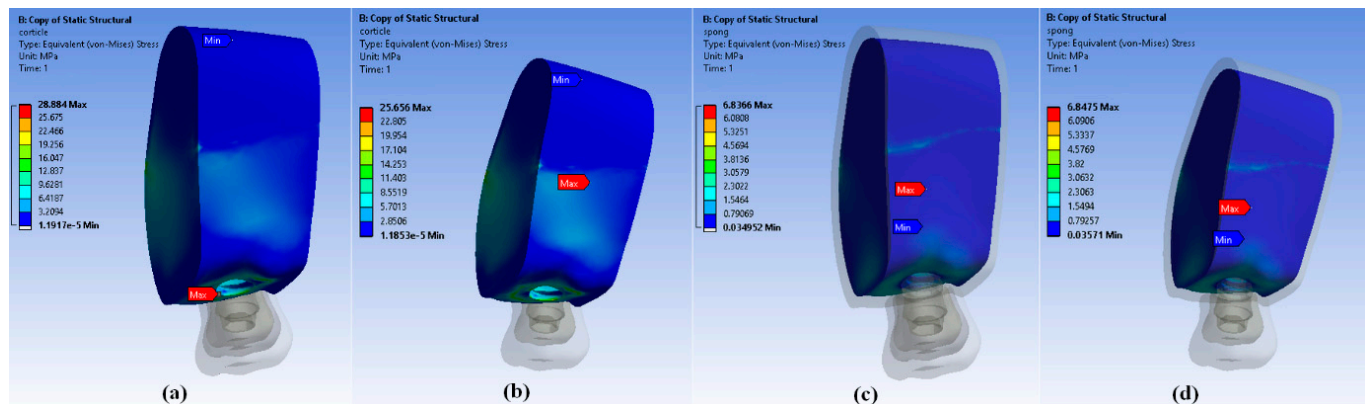


**Figure 9.** Stress distribution within supporting bone of D4 for vertical loading: (a) cortical bone in ZP and (b) cortical bone in MZ models; (c) cancellous bone in ZP; and (d) cortical bone in MZ models.

Figure 10 shows the maximum von Mises stresses within the cortical and cancellous bone regions under oblique loading conditions for different models (ZP and MZ). For the ZP model, the maximum von Mises stress observed in the cortical bone under oblique loading was 186 MPa. For the MZ model, the maximum stress observed in the cortical bone under oblique loading was 176.6 MPa [Figure 10a,b]. This indicates higher stress concentrations in the cortical bone for the ZP model compared to the MZ model when subjected to oblique loading forces. Similar to previous observations, the stress values in cancellous bone remained consistent across all models for both vertical and oblique loading forces. The maximum stress in the cancellous bone under vertical loading was 6.83 MPa for all models. Under oblique loading conditions, the maximum stress in cancellous bone was recorded as 13.6 MPa for all models [Figure 10c,d]. This consistency across models suggests that the stress levels in cancellous bone were uniform regardless of loading direction or model type.

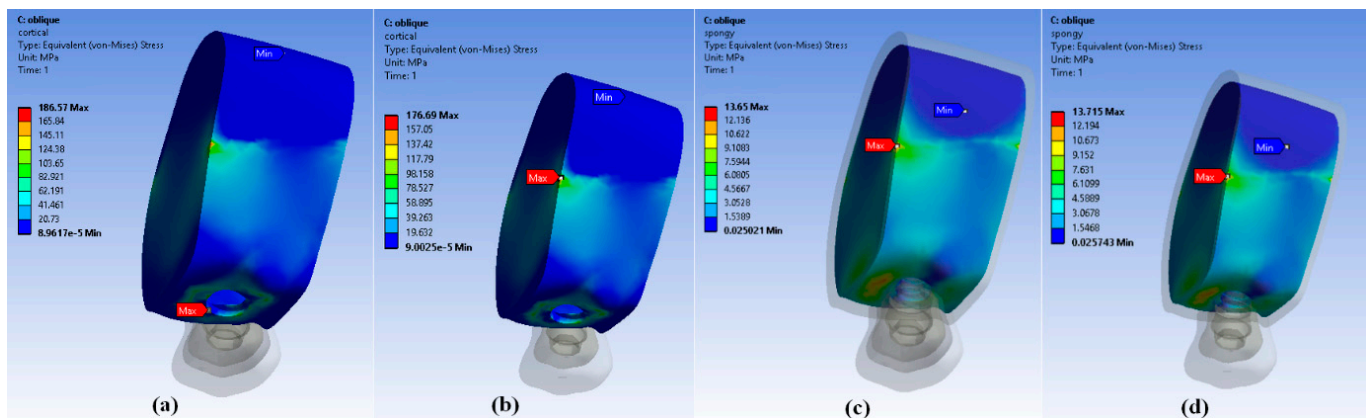


**Figure 10.** Stress distribution within supporting bone of D4: (a) vertical loading in ZP and (b) vertical loading MZ models; (c) oblique loading in ZP and (d) oblique loading in MZ models.

The results of stresses in the D2 and D4 bone are summarized in Tables 4–7 with respect to loading conditions on implant, cortical bone, and cancellous bone.

**Table 4.** Von Mises stresses (MPa) in ZP and MZ in D4 bone on vertical loading.

Location	ZP		MZ	
	Max	Min	Max	Min
Implant	116.24	0.5	109.6	0.53
Cortical bone	28.88	1.19	25.65	1.18
Cancellous bone	6.83	0.03	6.84	0.03

**Table 5.** Von Mises stresses (MPa) in ZP and MZ in D4 bone on oblique loading.

Location	ZP		MZ	
	Max	Min	Max	Min
Implant	1099	1.99	965.13	2.05
Cortical bone	186	8.9	176.6	9.00
Cancellous bone	13.6	0.02	13.7	0.02

**Table 6.** Von Mises stresses (MPa) in ZP and MZ in D2 bone on vertical loading.

Location	ZP		MZ	
	Max	Min	Max	Min
Implant	88.6	0.84	80.34	1.16
Cortical bone	21.77	0.0006	13.12	0.0007
Cancellous bone	5.30	0.03	4.417	0.02

**Table 7.** Von Mises stresses (MPa) in ZP and MZ in D2 bone on oblique loading.

Location	ZP		MZ	
	Max	Min	Max	Min
Implant	530.83	1.198	421.39	0.09
Cortical bone	132.8	0.0008	109.8	0.03
Cancellous bone	8.93	0.015	6.42	0.06

#### 4. Discussions

The current study utilizes finite element analysis to evaluate and compare the effect of In-Ceram zirconia (ZP) and monolithic zirconia prosthetic (MZ) materials on the distribution of stresses in implants and surrounding bone in maxillary and mandibular sections of bone. In a study conducted by Papavasiliou et al. [31], they found that oblique loads could increase stress by as much as 10-fold. Similar results were obtained with the present study, as shown in Figure 11, where the stresses with oblique loading were higher than vertical loading irrespective of the bone type and the prosthetic superstructure [32].

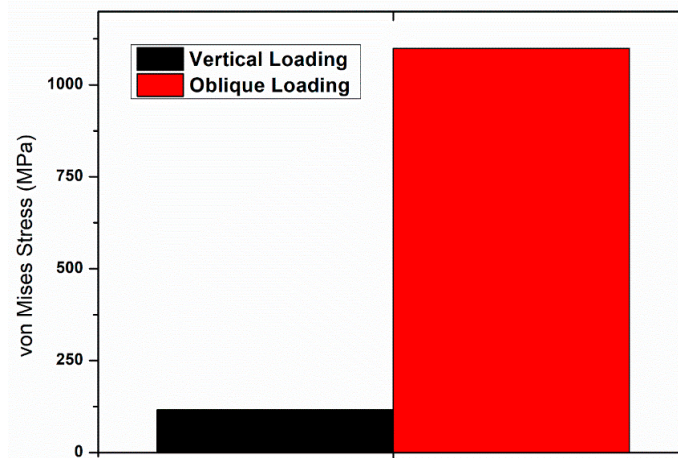


**Figure 11.** Comparison between vertical and oblique loading irrespective of bone quality and crown framework.

The current study utilizes finite element analysis to evaluate and compare the effect of In-Ceram zirconia (ZP) and monolithic zirconia prosthetic (ZP) materials on the distribution of stresses in implants and surrounding bone in maxillary and mandibular sections of bone.

Primary stability, which is one of the deciding factors for implant success, is dependent on bone quality. Higher implant success rates are seen in denser bone than porous bone, as cortical bone is more resistant to deformation due to a higher modulus of elasticity [33,34]. Based on the Hounsfield unit, Misch [35] classified bone density into four types—D1, D2, D3 and D4 [36]. It is proven that more stresses are generated in D3 and D4 bone compared to D1 and D2 bone [26,37]. In the present study, also, higher stress was seen in the D4 bone than in the D2 bone [Figure 12].

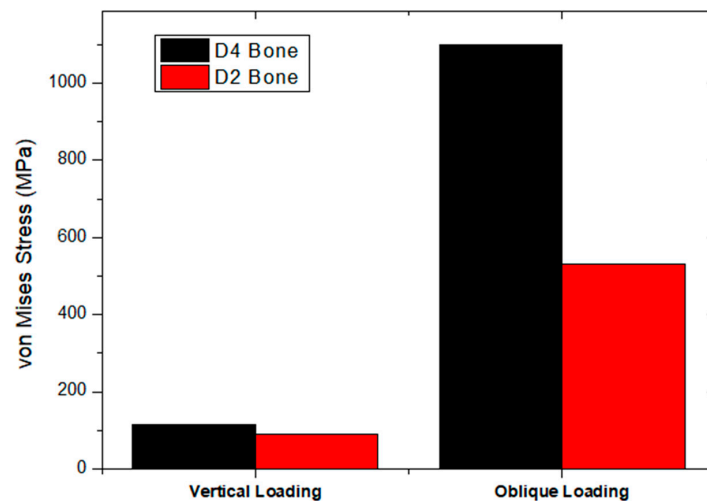


**Figure 12.** Comparison between D2 and D4 bone and the loading condition (vertical and oblique).

Osseointegration failure begins around the implant neck as more stresses are concentrated in the crestal region than the apical region [31,38]. Similar results were seen in the present study.

Even though there is a shift towards aesthetic restorations, all ceramics have a limited area of use as they are brittle. Hence, monolithic zirconia was introduced as it lacks porcelain veneering and therefore can be used even in case of parafunctional habits [39]. In the current study, different occlusal surface materials and frameworks generated different stresses in implants and the surrounding bone. The ZP model experienced higher maximum von Mises stresses in the cortical bone compared to the MZ model. This suggests that the ZP model exhibited greater stress concentrations within the cortical bone structure when subjected to vertical loading forces in the context of D4 bone density [Figure 13].

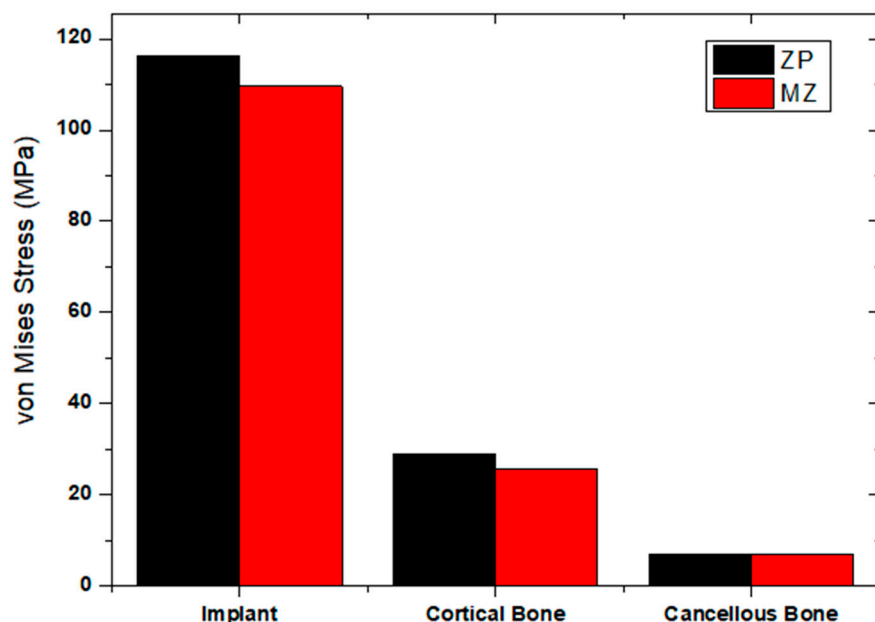


**Figure 13.** Comparison between ZP and MZ models in D4 bone on vertical loading.

The present study showed the least amount of von Mises stresses in the cancellous bone of D2 quality in the MZ model on vertical loading (4.417 MPa) (Figure 14). Maximum stresses were generated in the implant compared to the cortical bone because the Young's modulus of the implant (110 GPa) was higher than that of the bone (13.7 GPa). When the magnitude of stresses was compared in implants, among the ZP and MZ models, it was found that maximum von Mises stresses are concentrated in the ZP model in the D4 bone on oblique loading (1099 MPa) (Figure 15). This is because of the presence of porcelain veneer. Similar results were seen by Sevimay et al. [26]. Hence, it is concluded that physical and mechanical properties must also be considered, apart from aesthetics, for the long-term success of implants. The discrepancy in stress values between the ZP and MZ models suggests that the structural features or design of the ZP model may result in elevated stress concentrations within the cortical bone when exposed to oblique loading in D2 bone density scenarios [Figure 16].

#### Limitations

The work presented has several strengths, such as its comprehensive evaluation of stress distribution in dental implants using finite element analysis. However, there are notable limitations that should be considered. Firstly, the study relies heavily on numerical simulations (finite element analysis) rather than empirical data from clinical trials. While finite element analysis provides valuable insights, the actual clinical outcomes might differ due to various factors, including biological variations and patient-specific conditions. Additionally, the study assumes homogeneity and linear elastic behavior for all materials,

neglecting potential nonlinear and time-dependent characteristics. The material properties used in the analysis are derived from literature sources, introducing the possibility of variability and a lack of consideration for individual patient differences.

Furthermore, the study does not account for dynamic loading conditions that teeth and implants experience during functional activities. Chewing and biting forces are dynamic and multifactorial, and the static load of 200 N applied in this study may not fully represent real-world conditions.

In conclusion, while the finite element analysis provides valuable theoretical insights, the limitations, including the lack of clinical validation, simplified material properties, and static loading conditions, should be acknowledged. Future studies should aim to bridge the gap between numerical simulations and clinical reality by incorporating more realistic parameters and empirical data.

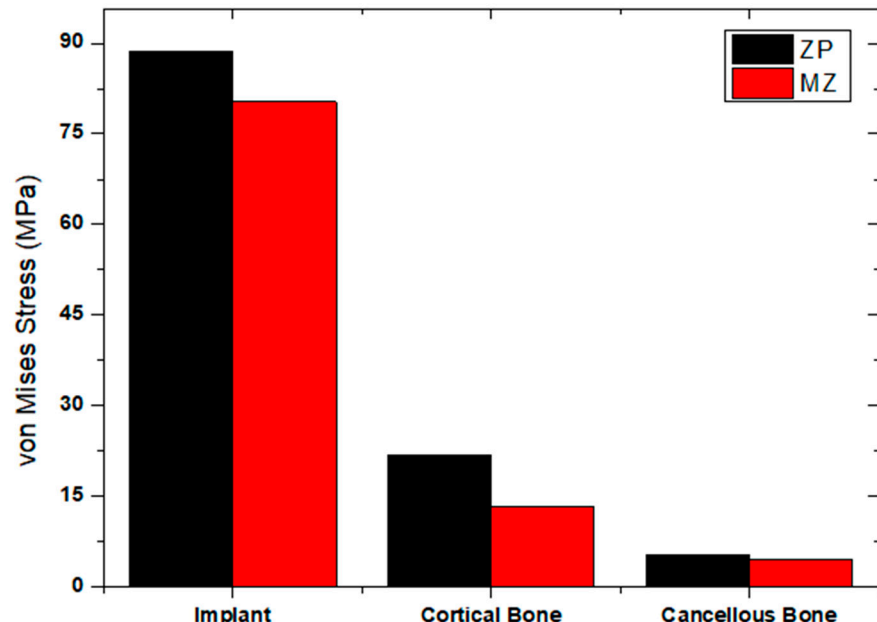


**Figure 14.** Comparison between ZP and MZ models in D2 bone on vertical loading.

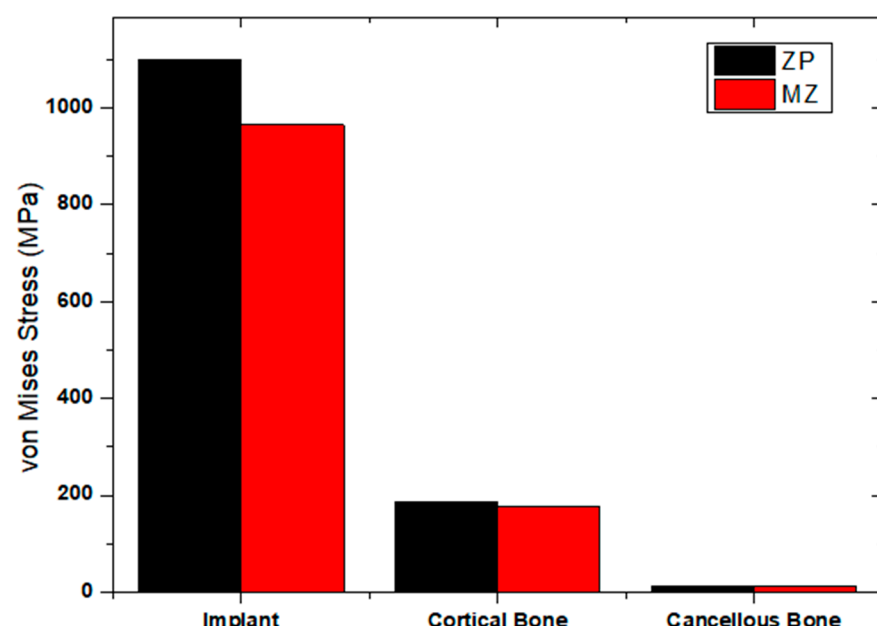


**Figure 15.** Comparison between ZP and MZ models in D4 bone on oblique loading.

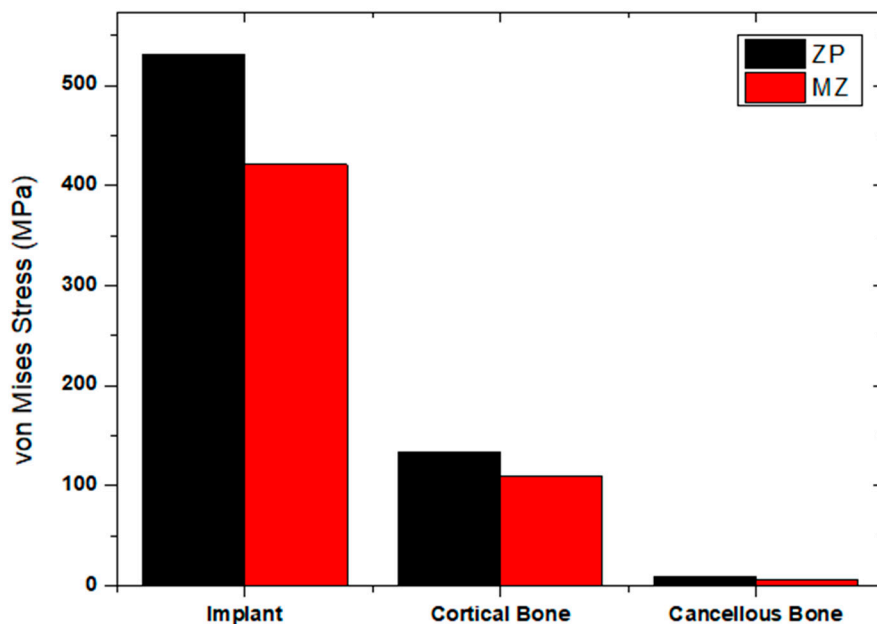


**Figure 16.** Comparison between ZP and MZ models in D2 bone on oblique loading.

## 5. Conclusions

Von Mises stress values were higher for oblique loading than vertical loading, irrespective of the superstructure material and bone density. For both vertical and oblique forces, the maxillary (D4) bone showed more stress than the mandibular (D2) bone. Stresses in implants were higher for the ZP model than MZ models irrespective of bone density and loading condition. For the D2 bone, stresses in cortical and cancellous bone for the ZP model were higher than the MZ model for both loading conditions. For the D4 bone, stresses in cortical bone were higher for the ZP model than the MZ model. However, in the case of cancellous bone stresses, they were equal for all the models for the vertical and oblique loading conditions.

**Author Contributions:** Conceptualization, L.G.K., C.K.N. and S.J.; methodology, G.M., A.E. and N.S.; software, L.G.K. and C.K.N.; validation, L.G.K., C.K.N. and N.S.; formal analysis, L.G.K.; investigation, C.K.N. and L.G.K.; resources, S.J., G.M., A.E. and N.S.; data curation, L.G.K. and C.K.N.; writing—original draft preparation, C.K.N. and L.G.K.; writing—review and editing, L.G.K., N.S., A.E. and N.S.; visualization, C.K.N.; supervision, S.J. and G.M.; project administration, S.J. All authors have read and agreed to the published version of the manuscript.

**Funding:** This research received no external funding.

**Institutional Review Board Statement:** Not applicable.

**Informed Consent Statement:** Not applicable.

**Data Availability Statement:** Data are contained within the article.

**Acknowledgments:** The authors would like to thank the Department of Aeronautical and Automobile Engineering, Manipal Institute of Technology, Manipal Academy for the computing resources provided to carry out this work.

**Conflicts of Interest:** The authors declare no conflicts of interest.

## References

- Shingade, A.; Dhatrak, P. Biomaterials used in dental applications to improve success rate of implantation: A review. *AIP Conf. Proc.* **2021**, *2358*, 090019. [[CrossRef](#)]
- Premnath, K.; Sridevi, J.; Kalavathy, N.; Nagarajani, P.; Sharmila, M.R. Evaluation of Stress Distribution in Bone of Different Densities Using Different Implant Designs: A Three-Dimensional Finite Element Analysis. *J. Indian Prosthodont. Soc.* **2013**, *13*, 555–559. [[CrossRef](#)] [[PubMed](#)]

3. Orlov, V.P.; Nashchekina, Y.A.; Nashchekin, A.V.; Ozeryanskaya, O.N.; Mirzametov, S.D.; Svistov, D.V. Biocompatibility of an interspinous implant made of titanium alloys. *Pediatr. Traumatol. Orthop. Reconstr. Surg.* **2022**, *10*, 407–415. [[CrossRef](#)]
4. Karthik, K.; Sivakumar; Sivaraj; Thangaswamy, V. Evaluation of implant success: A review of past and present concepts. *J. Pharm. Bioallied Sci.* **2013**, *5*, 117. [[CrossRef](#)]
5. Chugh, T.; Jain, A.K.; Jaiswal, R.K.; Mehrotra, P.; Mehrotra, R. Bone density and its importance in orthodontics. *J. Oral Biol. Craniofacial Res.* **2013**, *3*, 92–97. [[CrossRef](#)] [[PubMed](#)]
6. Sogo, M.; Ikebe, K.; Yang, T.; Wada, M.; Maeda, Y. Assessment of Bone Density in the Posterior Maxilla Based on Hounsfield Units to Enhance the Initial Stability of Implants. *Clin. Implant Dent. Relat. Res.* **2012**, *14*, e183–e187. [[CrossRef](#)] [[PubMed](#)]
7. Brunski, J.B. Biomaterials and biomechanics in dental implant design. *Int. J. Oral Maxillofac. Implants* **1988**, *3*, 85–97. [[PubMed](#)]
8. Lo Giudice, R.; Machado, P.S.; Dal Piva, A.M.d.O.; Tribst, J.P.M. Influence of Placement of Ultrashort Implant at Sub-Crestal, Crestal and Supra-Crestal Level with Titanium or Polyetheretherketone Hybrid Abutment: 3D Finite Element Analysis. *Prosthesis* **2023**, *5*, 721–732. [[CrossRef](#)]
9. Sailer, I.; Makarov, N.A.; Thoma, D.S.; Zwahlen, M.; Pjetursson, B.E. All-ceramic or metal-ceramic tooth-supported fixed dental prostheses (FDPs)? A systematic review of the survival and complication rates. Part I: Single crowns (SCs). *Dent. Mater.* **2015**, *31*, 603–623. [[CrossRef](#)]
10. Awan, M.R.U.; Asghar, H.; Raza, H.; Rasul, F.; Baig, M.S. Porcelain Metal Ceramic Crown Versus Porcelain Veneer. *Prof. Med. J.* **2018**, *25*, 709–713. [[CrossRef](#)]
11. Tavakolizadeh, S.; Yazdani, N.; Ghovali, R.; Mohammadi, A.; Beyabanki, E.; Kouliband, S. Fracture Resistance of Zirconia Restorations with Four Different Framework Designs. *Front. Dent.* **2023**, *20*, 2. [[CrossRef](#)] [[PubMed](#)]
12. Paracchini, L.; Barbieri, C.; Redaelli, M.; Di Croce, D.; Vincenzi, C.; Guarnieri, R. Finite Element Analysis of a New Dental Implant Design Optimized for the Desirable Stress Distribution in the Surrounding Bone Region. *Prosthesis* **2020**, *2*, 225–236. [[CrossRef](#)]
13. Kelly, J.; Benetti, P. Ceramic materials in dentistry: Historical evolution and current practice. *Aust. Dent. J.* **2011**, *56*, 84–96. [[CrossRef](#)] [[PubMed](#)]
14. Aljehani, W.A.; Kaki, A.S.; Al-Otaibi, M.T.; Tayeb, M.S.; Abunawas, O.M.; Alluhaidan, S.I.; Khalifa, R.M.; Binomran, A.A.; Shaikh, F.W.; Almadani, H.K. Advantages and limitations of monolithic zirconia restorations. *Int. J. Community Med. Public Health* **2023**, *10*, 845–849. [[CrossRef](#)]
15. Sannino, G.; Pozzi, A.; Schiavetti, R.; Barlattani, A. Stress distribution on a three-unit implant-supported zirconia framework. A 3D finite element analysis and fatigue test. *Oral Implantol.* **2012**, *5*, 11–20.
16. Eram, A.; Zuber, M.; Keni, L.G.; Naik, R.; Bhandary, S.; Amin, S.; Badruddin, I.A. Finite element analysis of immature teeth filled with MTA, Biodentine and Bioaggregate. *Comput. Methods Programs Biomed.* **2020**, *190*, 105356. [[CrossRef](#)] [[PubMed](#)]
17. Chethan, K.N.; Shyamasunder Bhat, N.; Satish Shenoy, B. Biomechanics of hip joint: A systematic review. *Int. J. Eng. Technol.* **2018**, *7*, 1672–1676. [[CrossRef](#)]
18. Chethan, K.N.; Shyamasunder Bhat, N.; Mohammad, Z.; Satish Shenoy, B. Evolution of different designs and wear studies in total hip prosthesis using finite element analysis: A review. *Cogent Eng.* **2022**, *9*, 2027081. [[CrossRef](#)]
19. Gutmann, C.; Shaikh, N.; Shenoy, B.S.; Shaymasunder Bhat, N.; Keni, L.G.; Chethan, K.N. Wear estimation of hip implants with varying chamfer geometry at the trunnion junction: A finite element analysis. *Biomed. Phys. Eng. Express* **2023**, *9*, 035004. [[CrossRef](#)]
20. de Aguiar Vilela Júnior, R.; Aranha, L.C.; Elias, C.N.; Martinez, E.F. In vitro analysis of prosthetic abutment and angulable frictional implant interface adaptation: Mechanical and microbiological study. *J. Biomech.* **2021**, *128*, 110733. [[CrossRef](#)]
21. Oancea, L.; Luca, I.; Radulescu, S.; Macris, A.; Ciocan, T. Systematic Review of In Vitro Studies on Distortion Generated by Intraoral Scanning Systems for Oral Rehabilitations with More Than Three Implants. *Prosthesis* **2023**, *5*, 1139–1152. [[CrossRef](#)]
22. Nelson, S.J.; Ash, M.M. *Wheeler's Dental Anatomy, Physiology, and Occlusion*; Saunders/Elsevier: Philadelphia, PA, USA, 2010.
23. Baggi, L.; Cappelloni, I.; Di Girolamo, M.; Maceri, F.; Vairo, G. The influence of implant diameter and length on stress distribution of osseointegrated implants related to crestal bone geometry: A three-dimensional finite element analysis. *J. Prosthet. Dent.* **2008**, *100*, 422–431. [[CrossRef](#)] [[PubMed](#)]
24. O'Brien, W.J. *Dental Materials and Their Selection*; Quintessence Publishing Company: New Malden, UK, 2002.
25. Guess, P.C.; Schultheis, S.; Bonfante, E.A.; Coelho, P.G.; Ferencz, J.L.; Silva, N.R.F.A. All-Ceramic Systems: Laboratory and Clinical Performance. *Dent. Clin. N. Am.* **2011**, *55*, 333–352. [[CrossRef](#)] [[PubMed](#)]
26. Sevimay, M.; Turhan, F.; Kılıçarslan, M.A.; Eskitascioğlu, G. Three-dimensional finite element analysis of the effect of different bone quality on stress distribution in an implant-supported crown. *J. Prosthet. Dent.* **2005**, *93*, 227–234. [[CrossRef](#)]
27. Cibirka, R.M.; Razzoog, M.E.; Lang, B.R.; Stohler, C.S. Determining the force absorption quotient for restorative materials used in implant occlusal surfaces. *J. Prosthet. Dent.* **1992**, *67*, 361–364. [[CrossRef](#)] [[PubMed](#)]
28. He, L.; Zhang, J.; Li, X.; Hu, H.; Lu, S.; Tang, Z. Irregular Implant Design Decreases Periimplant Stress and Strain Under Oblique Loading. *Implant Dent.* **2017**, *26*, 744–750. [[CrossRef](#)]
29. Pellizzer, E.P.; Verri, F.R.; de Moraes, S.L.D.; Falcón-Antenucci, R.M.; de Carvalho, P.S.P.; Noritomi, P.Y. Influence of the Implant Diameter With Different Sizes of Hexagon: Analysis by 3-Dimensional Finite Element Method. *J. Oral Implantol.* **2013**, *39*, 425–431. [[CrossRef](#)]
30. Morneburg, T.R.; Pröschel, P.A. Predicted incidence of occlusal errors in centric closing around arbitrary axes. *Int. J. Prosthodont.* **2002**, *15*, 358–364.

31. Papavasiliou, G.; Kamposiora, P.; Bayne, S.C.; Felton, D.A. Three-dimensional finite element analysis of stress-distribution around single tooth implants as a function of bony support, prosthesis type, and loading during function. *J. Prosthet. Dent.* **1996**, *76*, 633–640. [[CrossRef](#)]
32. Demenko, V.; Linetsky, I.; Nesvit, V.; Linetska, L.; Shevchenko, A. FE study of bone quality effect on load-carrying ability of dental implants. *Comput. Methods Biomed. Engin.* **2014**, *17*, 1751–1761. [[CrossRef](#)]
33. Ichikawa, T.; Kanitani, H.; Wigianto, R.; Kawamoto, N.; Matsumoto, N. Influence of bone quality on the stress distribution. *Clin. Oral Implants Res.* **1997**, *8*, 18–22. [[CrossRef](#)] [[PubMed](#)]
34. Holmes, D.C.; Loftus, J.T. Influence of bone quality on stress distribution for endosseous implants. *J. Oral Implantol.* **1997**, *23*, 104–111. [[PubMed](#)]
35. Misch, C.E. *Contemporary Implant Dentistry*; Elsevier Health Sciences: Amsterdam, The Netherlands, 2007.
36. Weinberg, L.A.; Kruger, B. A comparison of implant/prosthesis loading with four clinical variables. *Int. J. Prosthodont.* **1995**, *8*, 421–433. [[PubMed](#)]
37. Guven, S.; Demirci, F.; Yavuz, I.; Atalay, Y.; Ucan, M.C.; Asutay, F.; Altintas, E. Three-dimensional finite-element analysis of a single implant-supported zirconia framework and its effect on stress distribution in D4 (maxilla) and D2 (mandible) bone quality. *Biotechnol. Biotechnol. Equip.* **2015**, *29*, 984–990. [[CrossRef](#)]
38. Lin, C.-L.; Kuo, Y.-C.; Lin, T.-S. Effects of Dental Implant Length and Bone Quality on Biomechanical Responses in Bone Around Implants: A 3-D Non-Linear Finite Element Analysis. *Biomed. Eng. Appl. Basis Commun.* **2005**, *17*, 44–49. [[CrossRef](#)]
39. Sjögren, G.; Lantto, R.; Granberg, A.; Sundström, B.O.; Tillberg, A. Clinical examination of leucite-reinforced glass-ceramic crowns (Empress) in general practice: A retrospective study. *Int. J. Prosthodont.* **1999**, *12*, 122–128.

**Disclaimer/Publisher’s Note:** The statements, opinions and data contained in all publications are solely those of the individual author(s) and contributor(s) and not of MDPI and/or the editor(s). MDPI and/or the editor(s) disclaim responsibility for any injury to people or property resulting from any ideas, methods, instructions or products referred to in the content.